

# Real-time carotid plaque recognition from dynamic ultrasound videos based on artificial neural network

## Erkennung von Karotisplaques in Echtzeit aus dynamischen Ultraschallvideos anhand eines künstlichen neuronalen Netzes

**OPEN  
ACCESS**


### Authors

Yao Wei<sup>1†</sup>, Bin Yang<sup>2†</sup>, Ling Wei<sup>2</sup>, Jun Xue<sup>3</sup>, Yicheng Zhu<sup>4</sup>, Jianchu Li<sup>1</sup>, Mingwei Qin<sup>5</sup>, Shuyang Zhang<sup>6</sup>, Qing Dai<sup>1</sup>, Meng Yang<sup>1</sup>

### Affiliations

- 1 Department of Ultrasound, Peking Union Medical College Hospital, Dongcheng-qu, China
- 2 Institute for Internet Behavior, Tsinghua University, Beijing, China
- 3 Department of Echocardiography, China Meitan General Hospital, Beijing, China
- 4 Department of Neurology, Peking Union Medical College Hospital, Beijing, China
- 5 Telemedicine Center, Peking Union Medical College Hospital, Beijing, China
- 6 Department of Cardiology, Peking Union Medical College Hospital, Beijing, China

### Key words

Artificial intelligence, Carotid plaque, METHODS & TECHNIQUES, ultrasound, YOLOv4 neural network

received 06.06.2023

accepted after revision 15.09.2023

published online 2023

### Bibliography

Ultraschall in Med

DOI 10.1055/a-2180-8405

ISSN 0172-4614

© 2023. The Author(s).

This is an open access article published by Thieme under the terms of the Creative Commons Attribution-NonDerivative-NonCommercial-License, permitting copying and reproduction so long as the original work is given appropriate credit. Contents may not be used for commercial purposes, or adapted, remixed, transformed or built upon. (<https://creativecommons.org/licenses/by-nc-nd/4.0/>).

Georg Thieme Verlag KG, Rüdigerstraße 14,  
70469 Stuttgart, Germany

### Correspondence

Prof. Qing Dai

Department of Ultrasound, Peking Union Medical College Hospital, Shuai-Fu-Yuan Street 1, 100730 Dongcheng-qu, China  
qingdai\_2020@163.com

Prof. Meng Yang

Department of Ultrasound, Peking Union Medical College Hospital, Shuai-Fu-Yuan Street 1, 100730 Dongcheng-qu, China  
amengameng@hotmail.com

Additional material is available at <https://doi.org/10.1055/a-2180-8405>.

### ABSTRACT

**Purpose** Carotid ultrasound allows noninvasive assessment of vascular anatomy and function with real-time display. Based on the transfer learning method, a series of research results have been obtained on the optimal image recognition and analysis of static images. However, for carotid plaque recognition in real-time ultrasound detection. This study aims to establish an automatic recognition system, Be Easy to Use (BETU), for the real-time and synchronous diagnosis of carotid plaque from ultrasound videos based on an artificial neural network.

**Materials and Methods** 445 participants (mean age, 54.6 ± 7.8 years; 227 men) were evaluated. Radiologists labeled a total of 3259 segmented ultrasound images from 445 videos with the diagnosis of carotid plaque, 2725 images were collected as a training dataset, and 554 images as a testing dataset. The automatic plaque recognition system BETU was established based on an artificial neural network, and remote application on a 5G environment was performed to test its diagnostic performance.

**Results** The diagnostic accuracy of BETU (98.5 %) was consistent with the radiologist's (Kappa = 0.967, P < 0.001). Remote diagnostic feedback based on BETU-processed ultrasound videos could be obtained in 150 ms across a distance of

† These authors contributed equally.

1023 km between the ultrasound/BETU station and the consultation workstation.

**Conclusion** Based on the good performance of BETU in real-time plaque recognition from ultrasound videos, 5G plus Artificial intelligence (AI)-assisted ultrasound real-time carotid plaque screening was achieved, and the diagnosis was made.

## ZUSAMMENFASSUNG

**Hintergrund** Der Karotis-Ultraschall ermöglicht eine nicht invasive Beurteilung der Anatomie und Funktion von Gefäßen in Echtzeit. Auf der Grundlage der Transfer-Learning-Methode wurden viele Forschungsergebnisse zur optimalen Bildererkennung und Analyse statischer Bilder gewonnen. Für die Erkennung von Karotisplaques bestehen jedoch hohe Anforderungen an selbstentwickelte Algorithmen für die Echtzeit-Ultraschall-Erkennung. Ziel der Studie ist es, ein automatisches Erkennungssystem – Be-Easy-to-Use (BETU) – für die Echtzeit- und Synchrondiagnose von Karotisplaques aus Ultraschallvideos auf Basis eines künstlichen neuronalen Netzes zu entwickeln.

**Zu Material und Methoden** 445 Teilnehmer (Durchschnittsalter:  $54,6 \pm 7,8$  Jahre; 227 davon Männer) wurden untersucht. Radiologen stellten bei insgesamt 3259 segmentierten Ultraschallbildern aus 445 Videos die Diagnose „Karotisplaque“; 2725 Bilder wurden als Trainingsdatensatz und 554 Bilder als Testdatensatz gesammelt. Das automatische Plaque-Erkennungssystem BETU wurde auf Basis eines künstlichen neuronalen Netzes etabliert, und dessen diagnostische Leistung wurde durch eine Remote-Anwendung in einer 5G-Umgebung getestet.

**Ergebnisse** Die diagnostische Genauigkeit von BETU (98,5 %) stimmte mit der des Radiologen überein (Kappa = 0,967;  $p < 0,001$ ). Ein auf den BETU-prozessierten Ultraschallvideos basierendes Ferndiagnose-Feedback konnte in 150 ms über eine Entfernung von 1023 km zwischen dem Ultraschall-/BETU-System und dem Konsultations-Bildschirm erhalten werden.

**Schlussfolgerung** Basierend auf der guten Leistung von BETU bei der Echtzeit-Plaque-Erkennung aus Ultraschallvideos wurde ein 5G- plus durch künstliche Intelligenz (KI) gestütztes Echtzeit-Ultraschall-Screening von Karotisplaques durchgeführt und die Diagnose gestellt.

## Introduction

Atherosclerosis is a major cause of cerebrovascular diseases, and establishing its diagnosis entails a series of critical medical examinations to prevent cerebral and cardiovascular events [1, 2]. The intima-media thickness (IMT) of the common carotid artery (CCA) is one of the most common indicators of cardiovascular disease (CVD) development. Carotid IMT provides the first morphological evidence of atherosclerosis, whereas carotid plaques are stronger predictors of CVD than carotid IMT [3]. The risk of stroke increases with the severity of carotid stenosis [4, 5, 6]. The determination of IMT, delineation of the atherosclerotic carotid plaque, measurement of carotid artery diameter, and grading of its stenosis are important factors for the evaluation of atherosclerosis disease [7].

Magnetic resonance imaging (MRI) is currently the most well-established imaging modality for plaque characterization, with its high resolution and high sensitivity for identifying intraplaque hemorrhage, ulceration, lipid-rich necrotic core, and inflammation [8]. However, MRI is a time-consuming imaging modality. Moreover, protocols allowing high-resolution carotid plaque characterization are mainly used for research purposes [9]. CT also allows for high-resolution imaging and can accurately detect ulceration and calcification. However, CT scans involve radiation, and high-resolution CT images need contrast media imaging, which is not suitable for extensive repetitive screening and follow-up [8].

Carotid ultrasound (US) is one of the several imaging modalities allowing noninvasive assessment of vascular anatomy and function [10]. Considering that US is a time-saving, convenient, and economical modality, with real-time display, it is recommended as the first-line imaging modality for the assessment and screening of carotid IMT, plaque, and artery stenosis [11, 12]. However, in contrast to MRI and CT, US imaging needs to collect

dynamic images of different sections for real-time diagnosis, whereas other imaging modalities can establish the diagnosis based on static images. The acquisition and diagnosis of US images are highly dependent on the radiologist's experience. Unsatisfactory repeatability caused by the subjective dependence of operators is an important bottleneck for the standardization and homogenization of US imaging. Due to the complexity of medical images themselves, even experienced doctors may formulate different conclusions during the diagnosis process [13]. The introduction of high-resolution ultrasonography associated with computer-assisted methods for carotid plaque analysis has made it possible to standardize the ultrasonographic imaging characteristics. Therefore, it is of great importance and urgency to develop methods that can automatically identify carotid IMT and plaque based on static or dynamic US video imaging [7, 14].

Deep learning, especially convolutional neural networks (CNNs), has been applied to medical image processing in several studies, providing new ideas and methods for medical imaging diagnosis [15, 16, 17]. The high variability of ultrasonic images is a difficult problem in artificial intelligence (AI) imaging diagnosis. Recently, the main research field is focused on the thyroid, breast, and liver [18, 19]. Based on the transfer learning method, a series of research results have been obtained on the optimal image recognition and analysis of static images, and high accuracy has been achieved [20, 21, 22]. However, in real-time detection, the number of mainstream algorithms available for transfer learning is limited and is based on the You Only Look Once (YOLO) series algorithms. YOLO is a framework to solve the problem of target detection speed. As the recognized deep neural network in the field of AI, real-time analysis and efficiency are the most prominent features and advantages of YOLOv4.

This study aimed to establish an automatic recognition system, Be Easy to Use (BETU), for carotid plaques based on the framework of YOLOv4, achieving real-time and synchronous diagnosis during US examination to help sonographers screen and assess the burden of carotid plaques. In this study, cross-sectional images captured from the carotid US dynamic video were annotated by experienced sonographers to extract the features of carotid plaques. Based on the recognition of carotid plaques by BETU, we discussed the diagnostic performance of BETU and compared the recognition effect in images acquired from different ultrasonic devices.

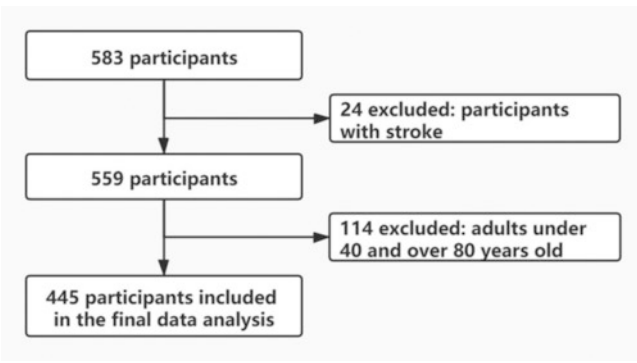
## Materials and Methods

### Study population

In this study, individuals with stroke and those who were less than 40 years old or above 80 years old were excluded (► Fig. 1). Finally, 445 participants were enrolled randomly in our retrospective study. The baseline characteristics of the study population are presented in ► Table 1. Institutional review board approval was obtained. All of the examinations were performed in accordance with relevant guidelines and regulations. Written informed consent was obtained from all participants.

### Instruments and data acquisition

All participants underwent carotid artery ultrasound and brain magnetic resonance examination. For all participants, US data for



► Fig. 1 Participant selection flowchart.

► Table 1 Characteristics of the study population (n = 445).

All participants	Mean ± SD or n (%)
<b>Demographic/medical history</b>	
Age, years	54.6 ± 7.8
Sex, % male	227 (51.0)
Hypertension, n (%)	194 (43.6)
Prior diabetes, n (%)	100 (22.5)

the CCA, internal carotid artery (ICA), and external carotid artery (ECA) were obtained in B-mode (grayscale) as longitudinal and transverse sections using an Esaote MyLab (Esaote, Genoa, Italy) with a linear 5–13-MHz transducer (LA523), Philips Lumify (Philips Healthcare, Eindhoven, Netherlands) with a linear 4–12-MHz transducer (L12–4), or Kangda i-M20 (Kangda Intercontinental Medical Equipment, Zhejiang, China) with a linear 4–12-MHz transducer (L154BH). Philips Lumify and Kangda i-M20 are portable ultrasonic devices. Each participant's left and right CCA, carotid bulb, and portions of the ICA and ECA were scanned by a trained sonographer (with more than 10 years of US experience). The cross-sectional US dynamic video frame rate was 20 frames per second (FPS).

The ultrasonic device was connected to a portable computer through a High-Definition Multimedia Interface. The portable computer collected US video in real time and transmitted the US dynamic videos to the server for calculation through the Real-Time Streaming Protocol. The actual deployed server configuration was as follows: processor Intel i5 8400 2.8GHz (six-core), 16G memory, 240G solid state drive, 4G graphics card GTX 1080ti, 500 W power supply, and built-in system CentOS7.4. After the server calculated the data, the returned results were displayed on a portable computer.

Brain MRI was obtained from a single 3 T Skyra scanner (Siemens, Erlangen, Germany). The 3D T1-weighted images using magnetization-prepared rapid gradient-echo sequence (repetition time [TR] 2,530 milliseconds, echo time [TE] 3.43 milliseconds, voxel size  $1 \times 1 \times 1.3 \text{ mm}^3$ , flip angle  $8^\circ$ , 144 sagittal slices), fluid-attenuated inversion recovery images (TR 8,500 milliseconds, TE 81 milliseconds, slice thickness 5 mm, gap 1 mm, 20 axial slices), susceptibility-weighted images (TR 20 milliseconds, TE 27 milliseconds, slice thickness 1.5 mm, flip angle  $15^\circ$ , 80 axial slices), and 3D time-of-flight magnetic resonance angiography (TR 21 milliseconds, TE 3.43 milliseconds, voxel size  $0.3 \times 0.3 \times 0.6 \text{ mm}^3$ , flip angle  $18^\circ$ , 136 axial slices) were included in the routine protocol.

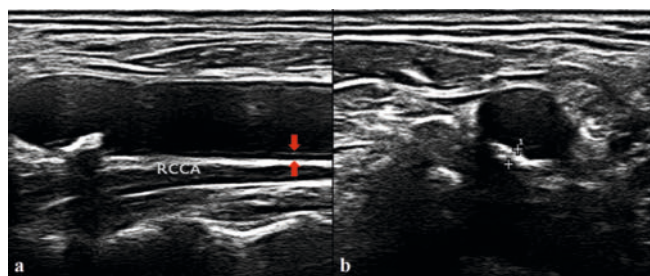
### Ultrasound characterization of atherosclerotic plaque

IMT is a double-line pattern, which consists of the leading edges of two anatomical boundaries. The lumen-intima and media-adventitia interfaces form the two boundaries. Based on the Standards for Carotid Ultrasound Examination in Healthy Subjects in China [23], plaques are focal structures encroaching into the arterial lumen of at least 0.5 mm or 50 % of the surrounding IMT value or that demonstrate a thickness > 1.5 mm measured from the intima-lumen interface to the media-adventitia interface (► Fig. 2) [24].

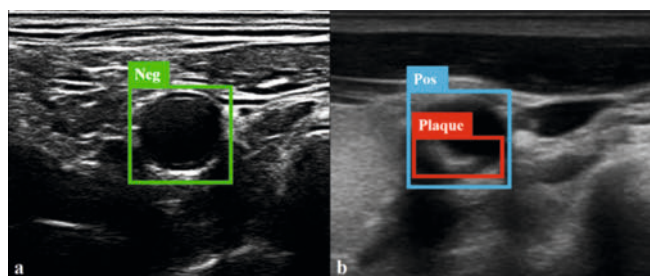
### Data preparation

Because of the color difference of the ultrasonic device, all the segmented US images from the videos were automatically converted to grayscale for training and recognition.

An anisotropic diffusion filter, an adaptive median filter, and other filtering algorithms were used to process US images to test whether they can improve accuracy. Finally, an adaptive brightness adjustment algorithm was applied to all images. Adjusting



► **Fig. 2** **a** Longitudinal view of the CCA. IMT is a double-line pattern, which consists of the leading edges of two anatomical boundaries. The lumen-intima and media-adventitia interfaces form the two boundaries (shown by the two red arrows). **b** Transverse view of the CCA. Plaques are focal structures encroaching into the arterial lumen with a thickness > 1.5 mm as measured from the intima-lumen interface to the media-adventitia interface (shown by the two '+' marks).



► **Fig. 3** **a** Negative. The carotid artery without plaque was identified by the green bounding box and labeled as Negative. **b** Positive. The carotid artery was identified by the blue bounding box and labeled as Positive, while the plaque was identified by the red bounding box.

the brightness ensured that the brightness of the image was consistent, and the image features were not lost.

According to the segmented US images, carotid plaques were manually labeled and confirmed by two senior US doctors (with more than 10 years of US experience).

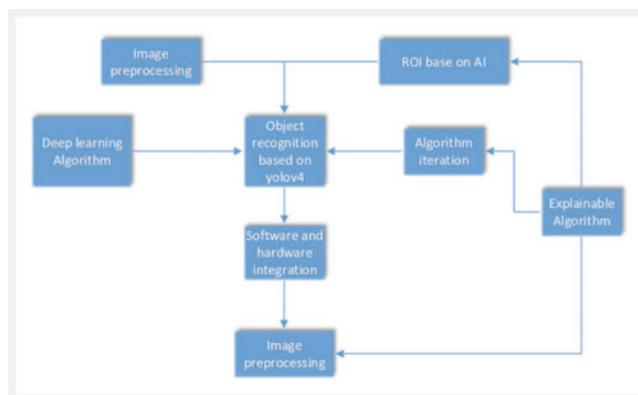
The doctors reviewed the US images and drew bounding boxes to identify the carotid arteries and plaques. Each carotid cross-sectional image was labeled as “negative” or “positive” with the plaque annotated in the image (► **Fig. 3**).

Different from other labeling methods, the plaque in the blood vessel and half of the blood vessels were marked with a red box as “plaque.” This will greatly reduce the loss of traditional methods for the identification of plaques with different shapes, enhance the understanding and recognition of intravascular plaque, and ultimately improve the recognition rate.

In total, 3259 carotid artery cross-sectional images acquired from 445 participants were labeled successfully.

### An artificial intelligence automatic image recognition model based on YOLOv4

The BETU system uses transfer learning as the main method to train the model through high-performance target detection algorithms such as YOLO and applies the training results to real-time



► **Fig. 4** System logic structure diagram.

US video processing tasks for the rapid recognition of blood vessels and vascular plaques. BETU also improves the dynamic recognition performance using a target tracking algorithm.

BETU processes the original US videos with automatic matching of the ultrasonic device, and only the area containing valid data is reserved for calculation. This can increase the recognition ability of BETU in plaque areas.

The cross-sectional dynamic US videos of each participant were stored in a database to be segmented automatically by the algorithm at 0.15-s intervals.

The core idea of the YOLO target recognition algorithm is to transform the target recognition problem into a regression problem, which achieves rapid target recognition with only one deep convolution network and high accuracy. YOLOv4 uses the improved DarkNet-53 [19] network based on ResNet as the feature extractor to improve the performance of small object recognition. (► **Fig. 4** and **Supplementary figure**).

The BETU system uses YOLOv4 as an algorithm for the rapid detection of blood vessels and vascular plaques. In total, 2725 carotid artery cross-sectional images were randomly collected as the training dataset. The remaining 554 images were collected as the testing dataset.

To solve the problem with regard to capturing and tracking the key features in the real-time recognition process of dynamic US videos, based on fast recognition, the BETU system tracks and displays the identified high-confidence feature targets through the target tracking technology, such as Kalman filtering, to improve the accuracy of recognition.

NVIDIA Tesla V100 graphics processing units (GPU) and GTX 1080Ti GPU were used for testing the dataset.

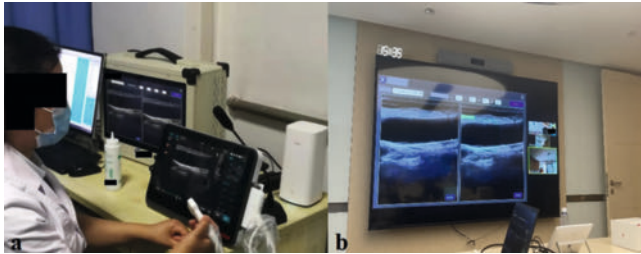
### Application based on the BETU system

After the algorithm verification is completed, the fifth-generation wireless system (5G) plus AI remote real-time assisted diagnostic testing of carotid artery US was conducted between two cities about 1023 km apart (► **Fig. 5**). The BETU system recognized the real-time dynamic ultrasound images that were sent to the higher level hospital based on the 5G network from community health service centers in another city.

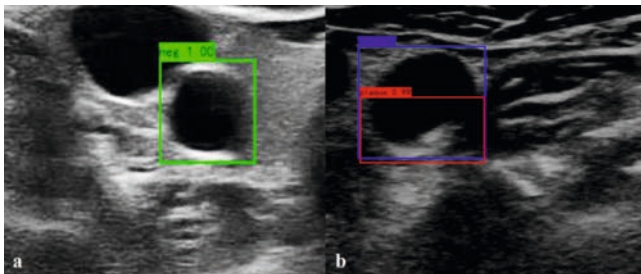


## Statistical analyses

The differences in the interpretations of plaque-positive and plaque-negative CCA from different diagnostic methods were tested using the chi-squared test. Based on the result confirmed by senior US doctors, the sensitivity, specificity, positive predictive value (PPV), negative predictive value (NPV), and accuracy were calculated to evaluate the diagnostic abilities of the BETU on CCA plaque. The kappa test was used to check for consistency.  $P < 0.05$  was considered statistically significant. The statistical software package SPSS 19.0 (IBM Corporation, Armonk, NY, USA) was used for all data analyses.



► **Fig. 5** Practical application for remote consultation between two cities across 1023 km in May 2021. **a** AI-powered carotid ultrasound screening and remote consultation in community health service centers of one city. **b** The remote consultation room and remote consultation screen in a higher-level hospital.



► **Fig. 6** The real-time results of the automatic recognition system. **a** Negative carotid was recognized automatically with the green bounding box and execution level of 1.00. **b** Positive carotid was recognized automatically with the blue bounding box and execution level of 1.00, and the plaque was recognized with the red bounding box and execution level of 0.99.

## Data Availability Statements

The data on which this article is based will be shared upon reasonable request to the corresponding author.

## Results

### Diagnostic performance measurements

In the 3259 training dataset images, 1586 positive and 1673 negative images were confirmed by senior US doctors.

In the 554 testing dataset images, the results were as follows: 288 positive and 266 negative images were confirmed by senior US doctors, whereas 287 positive and 267 negative images were recognized in real time by BETU (► **Fig. 6**). ► **Table 2** shows the results of the different device-sourced images recognized by the BETU. The results were confirmed by brain MRI (► **Fig. 7**). MRI can clearly show the lipid necrotic core, hemorrhage, calcification and other components of the plaque and the status of the fibrous cap. Different types of plaque have different appearances on MRI.

BETU and manual methods were consistent in the diagnosis of CCA plaques (kappa = 0.967,  $P < 0.001$ ).

The mean average precision of the BETU was 98.5 %. The BETU yielded an accuracy, sensitivity, specificity, PPV, and NPV of 98.5 % (95 % confidence interval [CI]: 0.97–0.99), 98.3 %, 98.5 %, 98.6 %, and 98.1 %, respectively.

Considering video segmentation, image scaling, engineering algorithms, and other time losses, the detection speed based on the NVIDIA Tesla V100 GPU was 39 FPS, which was higher than the frame rate of the original videos, whereas the detection speed based on the GTX 1080Ti GPU was 13 FPS.

### Be Easy to Use performance between different device-sourced images

The BETU yielded an accuracy, sensitivity, and specificity of 98.4 % (95 % CI: 0.97–1.0), 98.4 %, and 98.4 %; 96.2 % (95 % CI: 0.91–1.01), 95.0 %, and 96.9 %; and 99.2 % (95 % CI: 0.98–1.01), 98.8 %, and 100 % based on Esaote MyLab-sourced, Philips Lumify-sourced, and Kangda i-M20-sourced images, respectively (► **Table 3**).

Comparison of the BETU performance between the different device-sourced images suggested that there were no significant differences in accuracy, sensitivity, and specificity among the three device-sourced images ( $P = 0.545$ ,  $P = 0.339$ , and  $P = 0.493$ , respectively).

► **Table 2** Results of testing dataset.

Devices	Manual method		YOLOv4	
	Positive	Negative	Positive	Negative
MyLab (n = 375)	183	192	183	192
Lumify (n = 52)	20	32	20	32
i-M20 (n = 127)	85	42	84	43
N = 554	288	266	287	267

## Remote consultation application

With the advantages of 5G networks, such as high speed and low delay, the scanning terminal of the BETU device in a 5G environment can reach a transmission speed of milliseconds. After the actual business test, within 1023 km, ultrasound video data could be obtained, and assisted diagnosis results could be fed back within 150 milliseconds.

## Discussion

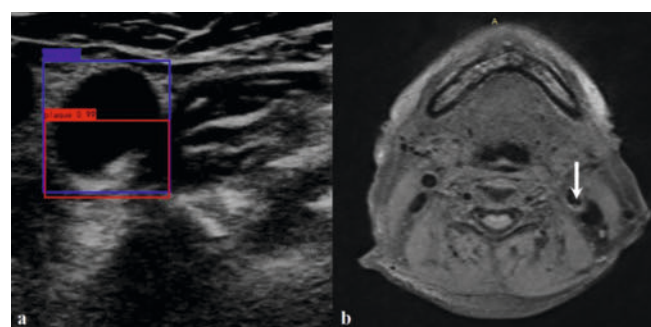
AI-powered US has become a more developed tool that can be commonly used in routine clinical applications in recent years because of the increased need for efficient and objective acquisition and evaluation of US images. Recently, the main research field has focused on the image analysis of static images from the thyroid, breast, and liver [25]. In real-time dynamic detection, the number of mainstream algorithms that can be used for transfer learning is limited and most of them are based on YOLO series algorithms. Compared with the traditional CNN for the recognition of carotid

plaque, real-time recognition of carotid plaque has rarely been studied [26, 27, 28].

In our study, the results were confirmed by brain MRI. BETU and manual methods were consistent in the diagnosis of carotid plaques ( $\kappa = 0.967$ ,  $P < 0.001$ ). This result is especially important in developing countries with a large population and unbalanced medical resources. An AI system requires only a short time (with millisecond resolution) for recognition. In reference to the results of the AI system, the diagnosis time of the radiologists can be effectively reduced, which simplifies CCA screening. Many studies have focused on the automatic method for the recognition of carotid plaques [14, 15, 26, 27, 28]. In several earlier studies, cumbersome image preprocessing, complex computer analysis, and lengthy computation time are required, which makes it impossible to recognize plaques in real time. In our model, the regions of interest (ROIs) were automatically labeled, and the plaques were identified with accuracy, sensitivity, and specificity comparable to those of experienced US doctors. Additionally, the model established in this study achieves rapid recognition, enables real-time and dynamic inspection in US examinations, and has broad potential for clinical applications.

The core of AI is big data, computing power, and algorithms. Due to the complexity of medical images themselves, even experienced doctors may formulate different conclusions during the diagnostic process [17]. For computing power, in the field of real-time detection, there are high requirements for strong data computing power, which is difficult for large ultrasonic devices or portable devices. For the algorithm, there are few mature frameworks for real-time detection (object recognition) for transfer learning. Without a solution to this problem, it is difficult to apply AI in clinical practice.

Compared to other complex deep learning algorithms for classification, YOLO has defects regarding accuracy. It is difficult for YOLO to achieve classification accuracy similar to other studies on static images based on other algorithms with greater than 98% accuracy [29]. In the BETU system, an iterative mechanism was added, and the training dataset was updated and retrained through the results verified by experienced doctors. The final ac-



► **Fig. 7** The plaque recognized by BETU was confirmed by brain MRI. **a** Positive carotid was recognized automatically with the blue bounding box and execution level of 1.00, as well as the plaque was recognized with the red bounding box and execution level of 0.99. **b** Carotid plaque was shown on brain MRI (↓).

► **Table 3** YOLOv4 performance between various device-sourced images and the difference.

	Devices			P
	MyLab (n = 375)	Lumify (n = 52)	i-M20 (n = 127)	
TP	180	19	84	
TN	189	31	42	
FP	3	1	0	
FN	3	1	1	
Accuracy	369/375 (98.4 %)	50/52 (96.2 %)	126/127 (99.2 %)	0.545
Sensitivity	180/183 (98.4 %)	19/20 (95.0 %)	84/85 (98.8 %)	0.339
Specificity	189/192 (98.4 %)	31/32 (96.9 %)	42/42 (100 %)	0.493

TP: True positive. TN: True negative. FP: False positive. FN: False negative.

curacy was increased by improving the interpretability of the program throughout the project.

To achieve real-time recognition and detection, the software with a response speed on the millisecond level is insufficient, and it is necessary to solve the problems of hardware support or efficient network transmission speed. Customized hardware can integrate portable US devices with an industrial control computer with a built-in professional GPU. A new type of portable US device that contains a recognition program without a network is expected to be developed. The problem of efficient network transmission speed can be solved on the server side based on a 5G wireless system.

This study reflects the advantages of ultrasound AI in real-time diagnosis. The 5G network can assist sonographers to achieve efficient carotid plaque screening and diagnosis in remote consultation. However, this study has some limitations. The selection of core algorithms is very important. With the continuous development of AI and machine learning, more efficient algorithms may appear in the future to replace the current algorithms. On the other hand, 5G is characterized by high speed and low delay. It is expected to be applied to ultrasonic remote diagnosis and treatment with the development of 5G technology. However, the current coverage is limited. The broadcast distance of the 5G network is shorter than that of the 4G network, and the cost of base station setup is higher, so there are still some difficulties in deploying 5G network in remote areas.

## Conclusion

BETU showed a good diagnostic performance in real-time plaque recognition from ultrasound videos. Based on the good performance of BETU, 5G plus artificial intelligence (AI)-assisted ultrasound real-time carotid plaque screening and diagnosis were achieved.

## Funding

National High Level Hospital Clinical Research Funding (2022-PUMCH-B-064,2022-PUMCH-C-009,2022-PUMCH-D-002) | National Natural Science Foundation of China (U22A2023, 62325112) | <http://dx.doi.org/10.13039/501100001809>

## Acknowledgement

Thanks are due to our colleagues who provided expertise that greatly assisted the research. Thanks are due to the Editage website for assistance with editing for proper English language, grammar, punctuation, spelling, and overall style.

## Conflict of Interest

The authors declare that they have no conflict of interest.

## References

- [1] Hodis HN, Mack WJ, LaBree L et al. The Role of Carotid Arterial Intima-Media Thickness in Predicting Clinical Coronary Events. *Ann Intern Med* 1998; 128 (4): 262–269. doi:10.7326/0003-4819-128-4-199802150-00002
- [2] O'Leary D, Polak J, Kronmal R et al. Carotid-artery intima and media thickness as a risk factor for myocardial infarction and stroke in older adults. *N Engl J Med* 1999; 340 (1): 14–22. doi:10.1056/NEJM199901073400103
- [3] Clarke R, Du H, Kurmi O et al. Burden of carotid artery atherosclerosis in Chinese adults: Implications for future risk of cardiovascular diseases. *Eur J Prev Cardiol* 2017; 24 (6): 647–656. doi:10.1177/2047487317689973
- [4] Clinical advisory: carotid endarterectomy for patients with asymptomatic internal carotid artery stenosis. *Stroke* 1994; 25 (12): 2523–2524. doi:10.1161/01.str.25.12.2523
- [5] Go AS, Mozaffarian D, Roger VL et al. Heart disease and stroke statistics-2013 update: a report from the American Heart Association. *Circulation* 2013; 127 (1): e6–e245. doi:10.1161/CIR.0b013e31828124ad
- [6] Rothwell PM, Gibson RJ, Slattery J et al. Prognostic value and reproducibility of measurements of carotid stenosis. A comparison of three methods on 1001 angiograms. European carotid surgery trialists' collaborative group. *Stroke* 1994; 25 (12): 2440–2444. doi:10.1161/01.str.25.12.2440
- [7] Loizou CP. A review of ultrasound common carotid artery image and video segmentation techniques. *Med Biol Eng Comput* 2014; 52 (12): 1073–1093. doi:10.1007/s11517-014-1203-5
- [8] Brinjikji W, Huston J 3rd, Rabinstein AA et al. Contemporary carotid imaging: from degree of stenosis to plaque vulnerability. *J Neurosurg* 2016; 124 (1): 27–42. doi:10.3171/2015.1.JNS142452
- [9] Roy-Cardinal MH, Destremes F, Soulez G et al. Assessment of carotid artery plaque components with machine learning classification using homodyned-K parametric maps and elastograms. *IEEE Trans Ultrason Ferroelectr Freq Control* 2019; 66 (3): 493–504. doi:10.1109/TUFFC.2018.2851846
- [10] Wei Y, Wang M, Gui Y et al. Carotid artery stiffness in rural adult Chinese: a cross-sectional analysis of the community-based China stroke cohort study. *BMJ Open* 2020; 10 (10): e036398. doi:10.1136/bmjopen-2019-036398
- [11] Greenland P, Alpert JS, Beller GA et al. 2010 ACCF/AHA guideline for assessment of cardiovascular risk in asymptomatic adults: a report of the American College of Cardiology Foundation/American Heart Association Task Force on Practice Guidelines. *J Am Coll Cardiol* 2010; 56 (25): e50–103. doi:10.1016/j.jacc.2010.09.001
- [12] Brott TG, Halperin JL, Abbara S et al. 2011 ASA/ACCF/AHA/AANN/AANS/ACR/ASNR/CNS/SAIP/SCAI/SIR/SNIS/SVM/SVS guideline on the management of patients with extracranial carotid and vertebral artery disease. A report of the American College of Cardiology Foundation/American Heart Association Task Force on Practice Guidelines, and the American Stroke Association, American Association of Neuroscience Nurses, American Association of Neurological Surgeons, American College of Radiology, American Society of Neuroradiology, Congress of Neurological Surgeons, Society of Atherosclerosis Imaging and Prevention, Society for Cardiovascular Angiography and Interventions, Society of Interventional Radiology, Society of NeuroInterventional Surgery, Society for Vascular Medicine, and Society for Vascular Surgery. *Circulation* 2011; 124 (4): e54–130. doi:10.1161/CIR.0b013e31820d8c98
- [13] Sun W, Zheng B, Huang X et al. Balance the nodule shape and surroundings: a new multichannel image based convolutional neural network scheme on lung nodule diagnosis. *Proc SPIE Medical Imaging* 2017; 10134: 101343L. doi:10.1117/12.2251297
- [14] Pedro LM, Pedro MM, Gonçalves I et al. Computer-assisted carotid plaque analysis: characteristics of plaques associated with cerebrovascular symptoms and cerebral infarction. *Eur J Vasc Endovasc Surg* 2000; 19 (2): 118–123. doi:10.1053/ejvs.1999.0952

- [15] Menchón-Lara RM, Sancho-Gómez JL, Bueno-Crespo A et al. Early-stage atherosclerosis detection using deep learning over carotid ultrasound images. *Applied Soft Computing* 2016; 49: 616–628. doi:10.1016/j.asoc.2016.08.055
- [16] Sun X, Wie WU, Peng WU et al. Recognition of Carotid Plaque in Ultrasonic Images Based on Deep Convolutional Neural Network. *China Medical Device Information* 2016; 22 (5): 4–8
- [17] Fang Lu, Fa Wu, Peijun Hu et al. Automatic 3 D liver location and segmentation via convolutional neural network and graph cut. *Int J Comput Assist Radiol Surg* 2017; 12 (2): 171–182. doi:10.1007/s11548-016-1467-3
- [18] Wang BS, Liu J B, Zhu Z et al. Artificial Intelligence in Ultrasound Imaging: Current Research and Applications. *Advanced Ultrasound in Diagnosis and Therapy* 2019; 3: 53–61. doi:10.37015/AUDT.2019.190811
- [19] Wang L, Yang S, Yang S et al. Automatic thyroid nodule recognition and diagnosis in ultrasound imaging with the YOLOv2 neural network. *World J Surg Oncol* 2019; 17 (1): 12. doi:10.1186/s12957-019-1558-z
- [20] Xue LY, Jiang ZY, Fu TT et al. Transfer learning radiomics based on multi-modal ultrasound imaging for staging liver fibrosis. *Eur Radiol* 2020; 30 (5): 2973–2983. doi:10.1007/s00330-019-06595-w
- [21] Zhuang Z, Kang Y, Raj ANJ et al. Breast ultrasound lesion classification based on image decomposition and transfer learning. *Med Phys* 2020; 47 (12): 6257–6269. doi:10.1002/mp.14510
- [22] Zhou H, Wang K, Tian J. Online Transfer Learning for Differential Diagnosis of Benign and Malignant Thyroid Nodules with Ultrasound Images. *IEEE Trans Biomed Eng* 2020; 67 (10): 2773–2780. doi:10.1109/TBME.2020.2971065
- [23] Standards for Carotid Ultrasound Examination in Healthy Subjects in China. *Chin J Health Manage* 2015; 9 (4): 254–260. doi:10.3760/cma.j.issn.1674-0815.2015.04.004
- [24] Touboul PJ, Hennerici MG, Meairs MG et al. Mannheim carotid intima-media thickness and plaque consensus (2004–2006–2011). An update on behalf of the advisory board of the 3rd, 4th and 5th watching the risk symposia, at the 13th, 15th and 20th European Stroke Conferences, Mannheim, Germany, 2004, Brussels, Belgium, 2006, and Hamburg, Germany, 2011. *Cerebrovasc Dis* 2012; 34 (4): 290–296. doi:10.1159/000343145
- [25] Akkus Z, Cai J, Boonrod A et al. A Survey of Deep-Learning Applications in Ultrasound: Artificial Intelligence-Powered Ultrasound for Improving Clinical Workflow. *J Am Coll Radiol* 2019; 16: 1318–1328. doi:10.1016/j.jacr.2019.06.004
- [26] Bonanno L, Sottile F, Ciarleo R et al. Automatic Algorithm for Segmentation of Atherosclerotic Carotid Plaque. *J Stroke Cerebrovasc Dis* 2017; 26 (2): 411–416. doi:10.1016/j.jstrokecerebrovasdis.2016.09.045
- [27] Lekadir K, Galimzianova A, Betriu A et al. A Convolutional Neural Network for Automatic Characterization of Plaque Composition in Carotid Ultrasound. *IEEE J Biomed Health Inform* 2017; 21 (1): 48–55. doi:10.1109/JBHI.2016.2631401
- [28] Chaudhry A, Hassan M, Khan A et al. Automatic active contour-based segmentation and classification of carotid artery ultrasound images. *J Digit Imaging* 2013; 26 (6): 1071–1081. doi:10.1007/s10278-012-9566-3
- [29] Redmon J, Divvala S, Girshick R et al. You Only Look Once: Unified, Real-Time Object Detection. *IEEE Conference on Computer Vision and Pattern Recognition (CVPR)* 2016: 779–788. doi:10.1109/CVPR.2016.91.